

Integrating Artificial Intelligence and Augmented Reality in Robotic Surgery: An Initial dVRK Study Using a Surgical Education Scenario

Yonghao Long, Jianfeng Cao, Anton Deguet, Russell H. Taylor, and Qi Dou

Abstract—Robot-assisted surgery has become progressively more and more popular due to its clinical advantages. In the meanwhile, the artificial intelligence and augmented reality in robotic surgery are developing rapidly and receive lots of attention. However, current methods have not discussed the coherent integration of AI and AR in robotic surgery. In this paper, we develop a novel system by seamlessly merging artificial intelligence module and augmented reality visualization to automatically generate the surgical guidance for robotic surgery education. Specifically, we first leverage reinforcement learning to learn from expert demonstration and then generate 3D guidance trajectory, providing prior context information of the surgical procedure. Along with other information such as text hint, the 3D trajectory is then overlaid in the stereo view of dVRK, where the user can perceive the 3D guidance and learn the procedure. The proposed system is evaluated through a preliminary experiment on surgical education task peg-transfer, which proves its feasibility and potential as the next generation of robot-assisted surgery education solution.

I. INTRODUCTION

Artificial intelligence (AI) and augmented reality (AR) are two important and increasingly essential techniques to be developed for next-generation robotic surgery. So far, AI and AR have individually focused on different perspectives. In specific, AI concentrates on recognizing and planning surgical activities in a way similar to what surgeons could do, based on computation and analysis of collected sensory data such as endoscopic videos [1]–[3] and robotic kinematics [4]–[6]. Recent advances of AI have substantially enhanced a number of tasks such as situation awareness of surgical procedures [7], [8] and automation of some actions with surgical robots [9], [10]. In the meanwhile, AR aims to augment the surgical environment in a way to facilitate surgeon’s operation and decision-making, based on visualization and integration of additional information that is computed offline or in real-time [11], [12]. Equipped with an immersive view in surgical robotic console, AR has shown effectiveness for the education of novice surgeons [13]–[15] and is envisaged to be very helpful if could be adopted intra-operatively [16].

Unfortunately, to date, the advantages of AI and AR have not been merged in a sensible way for robotic surgery. The intriguing combination of AI and AR emerges as a versatile topic and has been exemplified in a number of application

This project was supported by CUHK Shun Hing Institute of Advanced Engineering (project MMT-p5-20), Hong Kong RGC TRS Project No.T42-409/18-R, and InnoHK Multi-Scale Medical Robotics Center.

Y. Long, J. Cao and Q. Dou are with the Department of Computer Science and Engineering, The Chinese University of Hong Kong. A. Deguet and R. H. Taylor are with the Department of Computer Science, The Johns Hopkins University. *Corresponding author: Qi Dou (qidou@cuhk.edu.hk)*

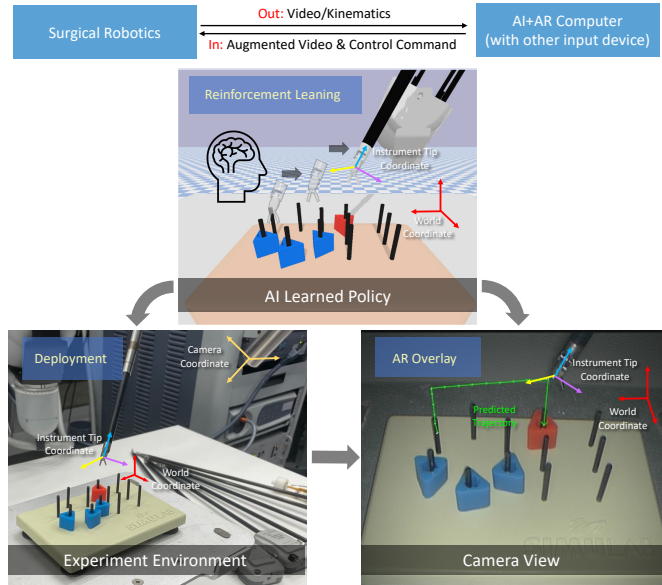


Fig. 1. The integrated framework of AI and AR in robotic surgery on surgical education scenario of peg-transfer. The AI learns policy in a stimulated environment based on reinforcement learning and predict the guidance trajectory, which will be further visualized in the dVRK stereo viewer in the form of AR overlaid trajectory.

scenarios, such as games [17], driver training [18], [19] and virtual patients [20], [21]. Conferring intelligence on AR not only can boost the virtual experience but also harnesses the strong power of learning-based algorithms in demanding tasks such as surgical education. However, there have been few attempts in combining AI and AR for surgical robots. Some authors [22]–[24] have proposed to use computer vision models to localize the anatomy regions of interest, and then superimpose the results in the view of camera. Nonetheless, these solutions only account for presenting existing clues perceptively, without shedding lights on human-like decision behaviors. Concurrently, reinforcement learning (RL) is widely recognized as an effective method for skill learning [25]–[28], but its potential is not fully exploited in the surgical robotics domain. One interesting scenario for exploring these issues is surgical education, in which the RL-based smart agent is expected to reason about surgical task and generate constructive guidelines for the novice. Such embodied intelligence is promising to significantly increase accessibility and reduce the cost of surgical training. Realisation of the intelligent guidance, in the form of AR visualization on surgical robotics platforms, could further enhance usability and user experience, yet how to achieve this goal remains unclear.

In this paper, we aim to seamlessly integrate AI and AR, by augmenting RL-driven instrument movement trajectories with real-time AR visualizations, and implement the pipeline for a surgical education scenario using da Vinci Research Kit (dVRK), as shown in Fig. 1. For the AI-enabled analysis, reinforcement learning is employed to learn a policy from the expert demonstration and through the interaction with the environment. Then the system can reason about the future action based on the current observation. This behavior can be embedded into an education process, where the automatically predicted actions could serve as helpful information to guide the trainee’s movement step-by-step. Subsequently, how to effectively visualize the information becomes very important, especially when incorporating with robotic platforms in real-time. We will demonstrate the feasibility of overlaying the 3D guidance trajectory within the stereo video via the dVRK console. By projecting the 3D location of the trajectory generated from RL policy to the stereo video frames in the dVRK console, we can vividly observe the surgical scene with overlaid trajectory for the education purpose. We have implemented and evaluated our method on the typical surgical education task of peg-transfer. To the best of our knowledge, this is the first work in exploring synergy of AI and AR with RL-based prediction and dVRK-based visualization for surgical education scenario. We hope to generate discussion and spark the potential of integrated benefits of AI and AR for surgical education and beyond.

II. RELATED WORK

A. Artificial Intelligence in Robotic Surgery

The application of artificial intelligence in robotic surgery has been actively studied over the last decade [29] since the da Vinci Surgical System being clinically introduced in 2000 [30]. Several topics have been found important and studied widely such as surgical instrument segmentation [31], gesture recognition [6], workflow recognition [1] and surgical scene reconstruction [32]. They could support intra-operative decision [33] and provide valuable database for surgical training and evaluation [34]–[36]. Although promising, these works just provide supplementary information without conceiving surgical plan, such as predicting the trajectories of the surgical instrument. Recently, the emergence of reinforcement learning opens the door to a new set of policy-based learning strategies [37]. The efficacy of reinforcement learning has been revealed in surgical gesture classification [38], [39], surgical scene understanding [40], [41] and robot learning [27], [42]. Through learning from expert demonstration, the RL agent could automatically generate meaningful solutions according to the task at hand. For example, in [27] and [28], the authors propose to use Deep Deterministic Policy Gradients (DDPG) with Behavior Cloning (BC) to conduct surgical task of bimanual needles regrasping and autonomous blood suction. Both of them demonstrate encouraging results, showing that RL-based framework may potentially alleviate the demands on expert’s guidance [43]–[45].

Apart from the above, there have been some works using AI for surgical education, such as providing metrics and performance feedback based on the training records [46]–[48] and differentiate expertise levels taking the stylistic characteristics into account [49]–[51]. But few of them consider its application to AR surgical education, where integrated AR and AI is highly demanded to guide the trainee vividly and automatically. Given the superiority of RL introduced above, it is compelling to integrate RL into AR as an essential AI module, for example, a decision-maker [52], [53], which encourages the AR system to generate content objectively.

B. Augmented Reality for Robotic Surgery

Augmented reality has been applied to robotic surgery in a variety of paradigms [12]. In intraoperative applications, augmentations are superimposed in real-time to offer assistance: (i) enhance depth perception [54]–[56], (ii) compensate tactile sensory [57], (iii) expand field of view [58], (iv) provide more intuitive human-machine interface [54], and (v) annotate helpful cues [59], [60]. Other applications utilize augmented reality for robotic surgery training [61]. The common displaying media of augmented reality for robotic surgery include the da Vinci console, the computer monitor, and head-mounted display [12]. For the purpose of surgical education, head-mounted display-based augmented reality is an advantageous medium as it enables 3D display and interactions for multiple users and the environment. Jarc et al. apply augmented reality to a clinical-like training scenario, where 3D semitransparent tools controlled by the proctor are augmented and overlaid in the trainee’s console as guidance [62]. User study involving seven proctor-trainee pairs is conducted, where they demonstrate the augmented tools as an effective mentoring approach. However, currently most of the AR system have not taken AI as the core component for generating and creating the context-aware information.

III. METHOD

A. Overall Framework

The whole system is based on the dVRK [63] platform, the first standard and general da Vinci surgical system that has been open-sourced and further developed for other researchers to explore [29]. It has been widely used for the research on surgical imaging and perception [6], control and hardware design [64], system simulation [65] and surgical task automation [66], which substantiate the high reliability and flexibility of the platform. In this work, we propose to fully leverage the advantage of dVRK to integrate the augmented reality and artificial intelligent to form a robotic surgery education system as shown in Fig. 2. In total, our framework consists of several parts as described below:

- 1) AI+AR Computing Server, as shown in Fig. 2 a): A high performance computer equipped with a high-end GPU for AR and AI algorithms deployment, which can acquire the stereo video and kinematics information from Patient Side Manipulator (PSM) and Endoscopic Camera Manipulator (ECM) on dVRK, receives input

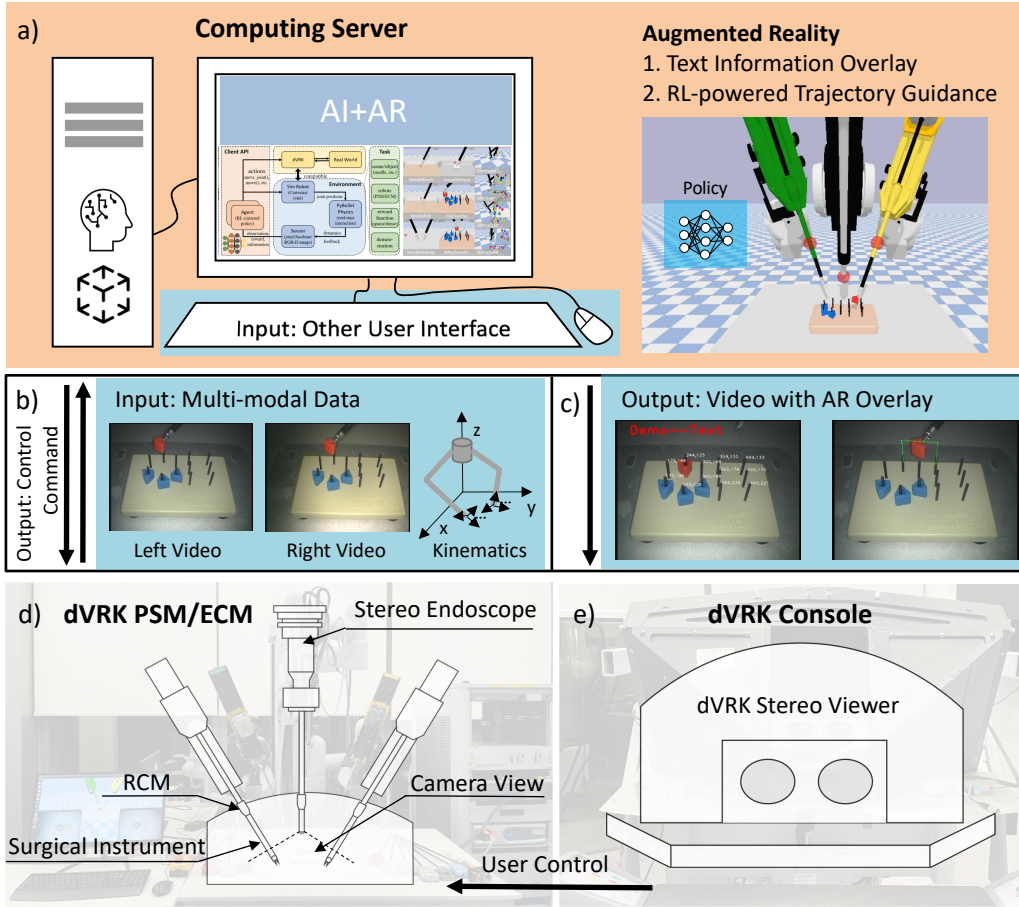


Fig. 2. The pipeline of our proposed robot-assisted surgery education system based on dVRK. The computing server a) can acquire the stereo video and kinematics b) from the dVRK PSM/ECM d) and input the command to control the movement of dVRK PSM. With the AR and AI algorithms, the computer can overlay the AI and AR information on the video c) and then import the augmented video to the dVRK console e) for user to view.

from other user interface, train and deploy RL policy or other AI framework and output the augmented video stream to monitor or other display devices.

- 2) Endoscope Video Acquisition and Kinematics Control: As depicted in Fig. 2 b) and d). The dVRK contains a stereo endoscope on ECM which can capture the stereo video stream for 3D sensing and perception. In this case, we collect the video signal from the dVRK stereo endoscope with a video capture card to convert the video signal to the USB video stream, which can be retrieved by the computer. By using the Application Programming Interface (API) provided by dVRK Robot Operating System (ROS) packages, users can acquire the kinematics information (including tool tip position, velocity, rotation) from two PSMs on dVRK and input kinematics to control the movement of the PSMs. Also, the PSMs can be control directly by user using hands in the dVRK console.
- 3) Displaying AR video with dVRK console: As depicted in Fig. 2 c) and e). Equipped with a stereo viewer in the dVRK console, users can view on the scene with overlaid AR and AI information from the computer in the surgical scenario. The stereo viewer can provide left and right views with disparity, where human can

perceive the surgical video and overlaid information with 3D feelings. This function is later developed into TilePro™ [67] in the following generation of da vinci surgical robot, which showcases the potential possibility of applying on the real robotic surgery.

B. Generating AI Guidance with Reinforcement Learning

Instead of guiding the novice surgeon by experienced expert, our work proposes to generate guidance through advanced reinforcement learning automatically. Considering the intriguing superiority of SurRoL [65] in leaning from demonstration and trials on dVRK, we attempt to incorporate it as our core AI module, learning and generating the guidance trajectory using the RL algorithm based on specific task.

SurRoL incorporates reinforcement learning to teach an intelligent agent to take interactive actions so that the cumulative reward can be maximized. While the agent takes action $a_t \in \mathcal{A}$ and interacts with the environment at state $s_t \in \mathcal{S}$, it receives reward $r_t \in \mathcal{R}$ based on whether the agent achieves the goal g at step t . From step $t = 0$ to $t = T$, the trajectory can be formulated as $\tau = \{s_0, r_0, a_0, s_1, r_1, a_1, \dots, s_T, r_T, a_T\}$. Besides, the transition $p(s_t|s_{t+1})$ is derived from the underlying physics engine.

For robotic surgery, we define a_t as six degrees of freedom, including position movement (d_x, d_y, d_z) in Cartesian space, orientation d_{yaw}/d_{pitch} in a top-down/vertical space setting and j for the open ($j \geq 0$) or close ($j < 0$) status of the jaw. Reinforcement learning targets on finding the policy π to generate action $a_t = \pi(s_t)$. To promote the learning process, the reward r_t is set to be goal-based, where the success function $f(s_t, g, a_t)$ would determine the reward r_t by checking whether a_t achieves the ground-truth status, such as 3D positions and 6D poses. Such scenario is similar to the attempting-feedback procedure in the surgical education. Finally, the target policy π is learned by maximizing the experimental expectation $\mathbb{E}_\pi[\sum_{t=0}^T \gamma^t r_t]$, where $\gamma \in [0, 1)$ denotes the discount factor to balance the agent's attention on distant future and immediate future. In specific, we opt for a sample efficient learning algorithm called hindsight experience replay (HER) [68] and combine it with Q-filtered behavior cloning. In practice, we will leverage a small amount of demonstration data generated from the scripted policies as the demonstration for imitation learning. It may have great potential to be extensively developed and learn from large amount of surgery data and then generate the AI-powered guidance for surgical education.

C. Real-time 3D Visualization by Augmented Reality

To facilitate the visualization result and form a more intuitive education, we propose to use the AR techniques to design a 3D visualization system for surgical robots.

1) *Different Coordinate System*: As an essential part of the AR system, the coordinates and the transformation among them serve as the basis of how we locate and align the AR information to camera view of the stereo endoscope. In our surgical education scenario, we denote the world coordinate as $\{W\}$, the coordinate of multiple objects in the experiment environment as $\{O_i\}$ with i indicating the index of the objects, Remote Center of Motion (RCM shown in Fig. 2 (b), which is a fixed base frame of the dVRK PSM during the operation) as $\{R\}$, the instrument tip as $\{P\}$ and the endoscope coordinate as $\{C\}$. And we use T_{src}^{dst} to denote as the transformation from source $\{src\}$ to destination coordinate $\{dst\}$. During the deployment, T_W^R are fixed and the same, and we manually place the objects in the same location as in the SurRoL. When given the kinematics information, we can compute the transformation of T_R^P using the forward kinematics theory and control the PSM to move the instrument tip to the target pose $\{P\}$ in the SurRoL and the real environment as below. If we have the transformation of the endoscope relative to the world T_W^C , we can calculate and get the position of the object relative to the endoscope T_C^O using the following equation:

$$T_C^O = T_W^O * T_C^W; \quad T_C^W = T_W^C^{-1} \quad (1)$$

2) *Human-involved Flexible Calibration*: Calibration process is to acquire the coordinate of the endoscope relative to the world T_W^C . It is an very important step [69] for AR, because it can align the AR information with the environment. Some methods have been proposed to calibrate

the hand-eye coordinate [70], [71], but they needs at least an expert on robotic vision who use the calibration board to complete the whole process. Using the QR code to automatically retrieve the coordinate is another attempt and solution [72], but we need to carefully take the detecting condition into consideration and it may be restricted in the surgical scene. In our work, we propose an user-friendly method to easily calibrate the endoscope coordinate, which is more suitable for surgical education scenario. Specifically, we will first define some specific points and collect the 3D position $[X_W^i, Y_W^i, Z_W^i]$ of these points from SurRoL (i denotes the point index). Then we manually locate the 2D location $[u_i, v_i]$ of these points in the image. We design an User Interface (UI) as depicted in Fig. 3, where users can easily locate and record the 2D location by clicking on the image using the mouse. According to the pinhole model of the camera, we can have the following equation:

$$\begin{bmatrix} u_i \\ v_i \\ 1 \end{bmatrix} = K * J * T_W^C \begin{bmatrix} X_W^i \\ Y_W^i \\ Z_W^i \\ 1 \end{bmatrix} \quad (2)$$

$$K = \begin{bmatrix} f_x & 0 & c_x \\ 0 & f_y & c_y \\ 0 & 0 & 1 \end{bmatrix}; \quad J = \begin{bmatrix} 1 & 0 & 0 & 0 \\ 0 & 1 & 0 & 0 \\ 0 & 0 & 1 & 0 \end{bmatrix}$$

where J represents the perspective projection model and K is the camera intrinsic matrix which can be straightforwardly acquired through [73]. To solve and acquire the solution for T_W^C , we leverage the stable method called iterative solvepnp algorithm [74]. It is based on Levenberg-Marquardt optimization which minimizes re-projection error and finds the best solution. The algorithm needs only 3 points for getting the solutions (more points contributes to better solution), which is convenient and efficient for surgical application.

3) *Augmented 3D Overlaying*: To overlay the 3D information on the image, we will first place the AR overlay information (3D) in the environment relative to the world coordinate T_W^{AR} , where we know the position $[X_W^{AR}, Y_W^{AR}, Z_W^{AR}]$. Then we will project the overlay information to the image using the projection equation same as the Eqn. (2). Specifically, we sometimes may need different views for AR overlaying. And we can use the proposed calibration method to calibrate the coordinate and overlay the new generated AR information relative to the new novel view. This is very promising as in the surgical education scenario, multiple views may enrich the information and help the surgeon to learn better.

D. Integrating AI and AR for Trajectory Guidance

With the AI and AR components introduced above, we further propose to integrate these two modules to form a AI-powered trajectory guidance with AR visualization. Firstly, the dVRK stereo endoscope will capture the stereo video from the surgical scenario and output for computing server. Then we will use the proposed calibration method to calculate and align the coordinate of the endoscope and world. We will then train the RL policy to learn on the specific tasks in the SurRoL. Given a well-learned policy



Fig. 3. Our proposed human-involved calibration process where we can flexibly locate the specific points on the peg board for calibrating.

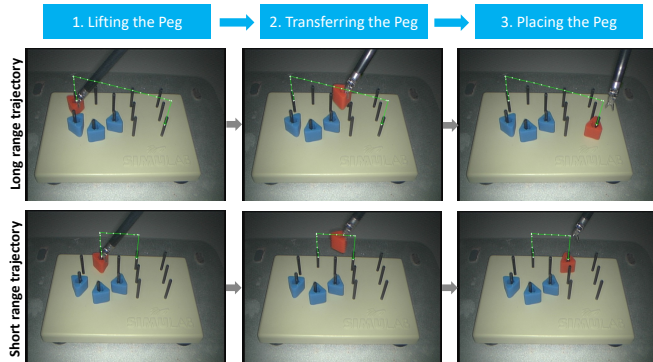


Fig. 4. Two trajectories overlay visualization results with long range transfer (top) and the short range transfer (bottom).

and providing with the known state of the environment or the observation, we can generate the predicted trajectory from the action, which is represented in the coordinate of the world. Afterwards, we can project the trajectory points to the video frames using the projection equation. By lining up the points, we can finally generate a trajectory guidance. With the augmented video displayed in the stereo viewer of dVRK console, the user can perceive the 3D AR trajectory guidance for the purpose of robotic surgery education.

IV. EXPERIMENT

To study the preliminary results of the proposed method, we choose the peg-transfer task as the experimental task in our work, which is one of the Fundamentals of Laparoscopic Surgery (FLS) tasks for surgical skills education [75]. In this experiment, we move the block from one peg to the other peg with one PSM on the dVRK. The whole process contains three procedures: 1) lifting the peg, 2) transferring the peg and 3) placing the peg, as depicted in Fig. 4. We train the RL policy on this task and generate the block transferring trajectory based on the trained model. Then we overlay the peg-transfer path as the AR trajectory on the stereo viewer for visualization.

We conduct the experiment on a computer using ubuntu 18.04 as the system, which is equipped with 8 cores 3.60GHz Intel® Xeon(R) W-2123 CPU, NVIDIA® TITAN RTX GPU and 16G RAM. All the algorithms are written in Python. The image resolution from the endoscope we use is 640×480 .

A. Reinforcement Learning on Peg-transfer

In this work, we follow the peg-transfer setting in SurRoL [65] where the goal tolerate distance is set as 0.5 cm in a workspace with size of 10 cm^2 . Each episode lasts for 50 timesteps. When the episode ends, PSM reaches out of the

TABLE I
THE EVALUATION OF Peg-Transfer ON SURRoL.

Distance	Trials	Success Rate (%)
Short range	463/500	92.6
Long range	401/500	80.2
All	864/1000	86.4

workspace or the peg-transfer is completed, the environment will be reset and the positions of initial peg and target peg will be resampled. Two evaluation settings are proposed, (1) short range: the block moved by user will not encounter any obstacle peg during the transfer; (2) long range: the block needs to avoid 1 to 3 pegs to finally reach the target peg, as these two situations are similar to simple and complicated surgical scenario for education. We randomly generate 100 scripted demonstrations for RL to imitate and train for 100 epochs in the training stage. In the testing stage, for each experiment, we conduct the peg transfer for 1000 trials (with 500 short range and 500 long range trials) and evaluate the success rate. We select top 3 performed RL policy and average their results. The results are shown in the Table I, where we can find that the RL policy can perform well on long range while achieving a higher performance on the short range peg-transfer with success rate 92.6%. Overall, our RL can achieve promising result with average success rate 86.4% on peg-transfer.

At the deployment stage, we export the complete predicted trajectory from the RL policy and input the trajectory location to control the PSM of real dVRK to conduct peg-transfer. We show a failure case from the long range setting in Fig. 5 a), where the block is not placed to the target peg properly because of the biased trajectory generated from the RL policy. Although there exists failure trial, the above results already bring out a lot of possibilities of applying more advanced RL algorithms on the complex robotic surgery education scenario.

B. Visualization and Analysis on the AR results

In the calibration process, we choose the top center points of the twelve pegs as the specific points $[u_i, v_i]$ for solving the coordinate of the endoscope. As we can see in Fig. 3, the specific points are located and shown in red dot. The point locations are shown next to these points with white text. After pointing out 12 points on the peg-transfer board, we can finish calibrating the coordinate.

As shown in Fig. 4, we show two cases from our experiments, with the top one showing the peg-transfer with long range distance and the bottom one showing the short range distance. In the experiment, we deploy our RL policy to generate the 3D trajectory and project the trajectory to the video frames. As we can see in the figure, the white dots in the image frame represent each action step in the trajectory, and the green lines represent the trajectory. It can be observed that our method can intuitively and accurately overlay the trajectory in the video frames, where the instrument tip will follow the overlaid trajectory visually in the experiment.

To further analyse the stability and precision of the calibration, we randomly find 5 new users with engineering

TABLE II

THE EVALUATION OF AR CALIBRATION ON Peg-Transfer SCENARIO.

Re-project error (pixel)	User1	User2	User3	User4	User5
Average value	0.77	1.02	0.70	0.61	0.71
Standard deviation	0.20	0.14	0.12	0.10	0.15

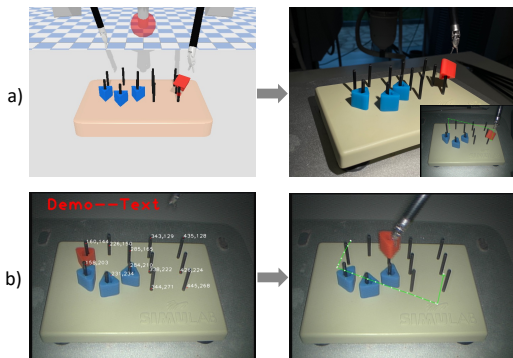


Fig. 5. The failure cases with (a) because of the biased trajectory generated from RL and (b) due to manually caused calibration error.

background to conduct the calibration process. We calculate the re-projection error (pixel) [76] based on twelve specific points on the pegs. Each user conducts 10 trials and we report the mean and standard deviation of the error in Table II. From the table we can find that average error is within 1 pixel (0.76) which is precise for the visualization purpose. Besides, we only observe one failure trial where the trajectory is calculated and projected to the wrong location due to the large error from manually locating the specific points, as shown in Fig. 5 b). The above results demonstrate the well performance of the calibration process and AR visualization for trajectory guidance on peg-transfer education scenario.

C. System Latency Study

As a systematic assessment of the whole pipeline, latency is more than important for a reliable and real-time system. In our work, we mainly focus on studying two different types of latency that may be introduced by the system. One is the video capturing and displaying latency, which is often caused by the delay of the video capture device, video signal transfer and the monitor. The other is overlaying latency, which is mainly caused by computing and projecting the points from 3D location to 2D image, as well as the time for drawing the information on the video frame.

To evaluate the video capturing and displaying delay, we place a tablet under the camera view of the endoscope which displays the timestamp on the screen. Then we capture the video from endoscope camera and display it on the screen of the computer. Afterwards, we take a photo using another camera, which will include both table screen and computer screen. The difference of two timestamps shown on two screens is the latency. The illustration can be seen in Fig. 6 (a). Finally, we find the average latency is around 161 milliseconds with standard deviation of 17 milliseconds from 100 samples. Which need to be mentioned is that the latency may vary when given different video capture equipment or monitor. According to some studies [77], [78] and our

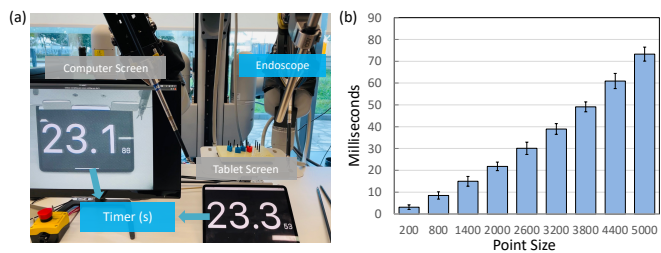


Fig. 6. (a) Illustration for evaluating video capturing and displaying latency and (b) chart showing the latency related to the point size.

own observation among all the trials, the latency is delicate enough that the human would not be able to perceive and will not significantly affect the operating.

To further evaluate the overlaying latency, we conduct an experiment which measures the computing time of overlaying (projecting 3D trajectory points to the video frames and visualize them). We evaluate the time cost when given different size of trajectory points (200-5000), as shown in Fig. 6 (b), where we randomly generate the 3D locations of these points and repeat the experiment for 300 times. Finally we report the average and standard deviation of the time cost. From the figure we can observe that when given more points, the computation time may increase showing exponential growth. When around or less than 2600 points, we can achieve the real-time process (> 30 Hz). In our peg transfer scenario, the RL will generate around 100 trajectory points which cost just about 1 ms for projecting and overlaying, it is more than enough for a real-time visualization. According to the above results, our designed system can efficiently overlay the trajectory on video frames forming a real-time AR visualization, which has great potential for more complicated real-time AR robotic surgery education scenario.

V. CONCLUSIONS AND FUTURE WORK

In this work, we confer the intelligence on AR by integrating AI module as a decision-maker for generating trajectory. The AI module with reinforcement learning is leveraged to learn policy-based operation and dynamically generate the trajectory based on user's task. To provide an immersive visualization and facilitate intuitive education, the trajectory plan is further projected and overlaid onto the stereo video, assisting the trainee to perceive the intelligent guidelines in 3D AR. A simple yet effective calibration with human-computer interaction is also designed to realize coordinate calibration through an user interface. We conduct the experiment with the surgical training on task peg-transfer, which demonstrates the feasibility and potential of AI-powered AR for robotic surgery education.

In our future work, we shall further exploit how to design and incorporate more AI and AR modules into the system, such as virtual tool guidance, overlaying the result of surgical workflow recognition and instrument segmentation. Furthermore, we shall integrate network communication for realizing a remote surgery education. Methods of measuring the operation of surgeon compared to the generated 'expert' trajectory and user study may also be included for evaluating the effectiveness of the proposed system.

REFERENCES

- [1] Y. Jin, Y. Long, C. Chen, Z. Zhao, Q. Dou, and P.-A. Heng, "Temporal memory relation network for workflow recognition from surgical video," *IEEE Transactions on Medical Imaging*, 2021.
- [2] B. Zhang, A. Ghanem, A. Simes, H. Choi, A. Yoo, and A. Min, "Swnet: Surgical workflow recognition with deep convolutional network," in *Medical Imaging with Deep Learning*, 2021.
- [3] B. van Amsterdam, M. J. Clarkson, and D. Stoyanov, "Gesture recognition in robotic surgery: A review," *IEEE Transactions on Biomedical Engineering*, vol. 68, no. 6, pp. 2021–2035, 2021.
- [4] B. v. Amsterdam, M. J. Clarkson, and D. Stoyanov, "Multi-task recurrent neural network for surgical gesture recognition and progress prediction," in *2020 IEEE International Conference on Robotics and Automation (ICRA)*. IEEE, 2020, pp. 1380–1386.
- [5] Y.-H. Su, K. Huang, and B. Hannaford, "Real-time vision-based surgical tool segmentation with robot kinematics prior," in *2018 International Symposium on Medical Robotics (ISMR)*. IEEE, 2018, pp. 1–6.
- [6] Y. Long, J. Y. Wu, B. Lu, Y. Jin, M. Unberath, Y.-H. Liu, P. A. Heng, and Q. Dou, "Relational graph learning on visual and kinematics embeddings for accurate gesture recognition in robotic surgery," in *2021 IEEE International Conference on Robotics and Automation (ICRA)*. IEEE, 2021, pp. 13 346–13 353.
- [7] C. R. Garrow, K.-F. Kowalewski, L. Li, M. Wagner, M. W. Schmidt, S. Engelhardt, D. A. Hashimoto, H. G. Kenngott, S. Bodenstedt, S. Speidel, *et al.*, "Machine learning for surgical phase recognition: a systematic review," *Annals of Surgery*, vol. 273, no. 4, pp. 684–693, 2021.
- [8] A. Huauhmé, D. Sarikaya, K. L. Mut, F. Despinoy, Y. Long, Q. Dou, C.-B. Chng, W. Lin, S. Kondo, L. Bravo-Sánchez, *et al.*, "Micro-surgical anastomose workflow recognition challenge report," *arXiv preprint arXiv:2103.13111*, 2021.
- [9] B. van Amsterdam, M. Clarkson, and D. Stoyanov, "Gesture recognition in robotic surgery: a review," *IEEE Transactions on Biomedical Engineering*, 2021.
- [10] H. Huynhnguyen and U. A. Buy, "Toward gesture recognition in robot-assisted surgical procedures," in *2020 2nd International Conference on Societal Automation (SA)*. IEEE, 2021, pp. 1–4.
- [11] F. Volonté, N. C. Buchs, F. Pugin, J. Spaltenstein, B. Schiltz, M. Jung, M. Hagen, O. Ratib, and P. Morel, "Augmented reality to the rescue of the minimally invasive surgeon. the usefulness of the interposition of stereoscopic images in the da vinci™ robotic console," *The International Journal of Medical Robotics and Computer Assisted Surgery*, vol. 9, no. 3, pp. e34–e38, 2013.
- [12] L. Qian, J. Y. Wu, S. P. DiMaio, N. Navab, and P. Kazanzides, "A review of augmented reality in robotic-assisted surgery," *IEEE Transactions on Medical Robotics and Bionics*, vol. 2, no. 1, pp. 1–16, 2019.
- [13] S. Sheik-Ali, H. Edgcombe, and C. Paton, "Next-generation virtual and augmented reality in surgical education: a narrative review," *Surgical technology international*, vol. 33, 2019.
- [14] E. Z. Barsom, M. Graafland, and M. P. Schijven, "Systematic review on the effectiveness of augmented reality applications in medical training," *Surgical endoscopy*, vol. 30, no. 10, pp. 4174–4183, 2016.
- [15] R. R. McKnight, C. A. Pean, J. S. Buck, J. S. Hwang, J. R. Hsu, and S. N. Pierrie, "Virtual reality and augmented reality—translating surgical training into surgical technique," *Current Reviews in Musculoskeletal Medicine*, pp. 1–12, 2020.
- [16] R. Londei, M. Esposito, B. Diotte, S. Weidert, E. Euler, P. Thaller, N. Navab, and P. Fallavollita, "Intra-operative augmented reality in distal locking," *International journal of computer assisted radiology and surgery*, vol. 10, no. 9, pp. 1395–1403, 2015.
- [17] E. Turan and G. Çetin, "Using artificial intelligence for modeling of the realistic animal behaviors in a virtual island," *Computer Standards & Interfaces*, vol. 66, p. 103361, 2019.
- [18] J. L. Gabbard, M. Smith, K. Tanous, H. Kim, and B. Jonas, "Ar drivesim: An immersive driving simulator for augmented reality head-up display research," *Frontiers in Robotics and AI*, vol. 6, p. 98, 2019.
- [19] R. G. Boboc, F. Gîrbacia, and E. V. Butilă, "The application of augmented reality in the automotive industry: A systematic literature review," *Applied Sciences*, vol. 10, no. 12, p. 4259, 2020.
- [20] S. Daher, J. Hochreiter, R. Schubert, L. Gonzalez, J. Cendan, M. Anderson, D. A. Diaz, and G. F. Welch, "The physical-virtual patient simulator: A physical human form with virtual appearance and behavior," *Simulation in Healthcare*, vol. 15, no. 2, pp. 115–121, 2020.
- [21] L. Gonzalez, S. Daher, and G. Welch, "Neurological assessment using a physical-virtual patient (pvp)," *Simulation & Gaming*, vol. 51, no. 6, pp. 802–818, 2020.
- [22] L. Tanzi, P. Piazzolla, F. Porpiglia, and E. Vezzetti, "Real-time deep learning semantic segmentation during intra-operative surgery for 3d augmented reality assistance," *International Journal of Computer Assisted Radiology and Surgery*, vol. 16, no. 9, pp. 1435–1445, 2021.
- [23] J. Pan, W. Liu, P. Ge, F. Li, W. Shi, L. Jia, and H. Qin, "Real-time segmentation and tracking of excised corneal contour by deep neural networks for dalk surgical navigation," *Computer Methods and Programs in Biomedicine*, vol. 197, p. 105679, 2020.
- [24] A. H. Sadeghi, A. P. Maat, Y. J. Taverne, R. Cornelissen, A.-M. C. Dingemans, A. J. Bogers, and E. A. Mahtab, "Virtual reality and artificial intelligence for 3-dimensional planning of lung segmentectomies," *JTCVS Techniques*, 2021.
- [25] A. Amini, I. Gilitschenski, J. Phillips, J. Moseyko, R. Banerjee, S. Karaman, and D. Rus, "Learning robust control policies for end-to-end autonomous driving from data-driven simulation," *IEEE Robotics and Automation Letters*, vol. 5, no. 2, pp. 1143–1150, 2020.
- [26] K. Kurach, A. Raichuk, P. Stańczyk, M. Zajac, O. Bachem, L. Espeholt, C. Riquelme, D. Vincent, M. Michalski, O. Bousquet, *et al.*, "Google research football: A novel reinforcement learning environment," *arXiv preprint arXiv:1907.11180*, 2019.
- [27] Z.-Y. Chiu, F. Richter, E. K. Funk, R. K. Orosco, and M. C. Yip, "Bimanual regrasping for suture needles using reinforcement learning for rapid motion planning," in *2021 IEEE International Conference on Robotics and Automation (ICRA)*. IEEE, 2021, pp. 7737–7743.
- [28] F. Richter, R. K. Orosco, and M. C. Yip, "Open-sourced reinforcement learning environments for surgical robotics," *arXiv preprint arXiv:1903.02090*, 2019.
- [29] C. D'Ettorre, A. Mariani, A. Stilli, P. Valdastrì, A. Deguet, P. Kazanzides, R. H. Taylor, G. S. Fischer, S. P. DiMaio, A. Menciassi, *et al.*, "Accelerating surgical robotics research: Reviewing 10 years of research with the dvrk," *arXiv preprint arXiv:2104.09869*, 2021.
- [30] P. Kazanzides, Z. Chen, A. Deguet, G. S. Fischer, R. H. Taylor, and S. P. DiMaio, "An open-source research kit for the da vinci® surgical system," in *2014 IEEE international conference on robotics and automation (ICRA)*. IEEE, 2014, pp. 6434–6439.
- [31] Z. Zhao, Y. Jin, X. Gao, Q. Dou, and P.-A. Heng, "Learning motion flows for semi-supervised instrument segmentation from robotic surgical video," in *International Conference on Medical Image Computing and Computer-Assisted Intervention*. Springer, 2020, pp. 679–689.
- [32] Y. Long, Z. Li, C. H. Yee, C. F. Ng, R. H. Taylor, M. Unberath, and Q. Dou, "E-dssr: efficient dynamic surgical scene reconstruction with transformer-based stereoscopic depth perception," in *International Conference on Medical Image Computing and Computer-Assisted Intervention*. Springer, 2021, pp. 415–425.
- [33] T. Blum, H. Feußner, and N. Navab, "Modeling and segmentation of surgical workflow from laparoscopic video," in *International Conference on Medical Image Computing and Computer-Assisted Intervention*. Springer, 2010, pp. 400–407.
- [34] N. Padov, T. Blum, S.-A. Ahmadi, H. Feussner, M.-O. Berger, and N. Navab, "Statistical modeling and recognition of surgical workflow," *Medical image analysis*, vol. 16, no. 3, pp. 632–641, 2012.
- [35] A. Nara, K. Izumi, H. Iseki, T. Suzuki, K. Nambu, and Y. Sakurai, "Surgical workflow analysis based on staff's trajectory patterns," in *M2CAI workshop, MICCAI, London, 2009*.
- [36] T. Neumuth, "Surgical process modeling," *Innovative surgical sciences*, vol. 2, no. 3, pp. 123–137, 2017.
- [37] A. Rakhsha, G. Radanovic, R. Devidez, X. Zhu, and A. Singla, "Policy teaching via environment poisoning: Training-time adversarial attacks against reinforcement learning," in *International Conference on Machine Learning*. PMLR, 2020, pp. 7974–7984.
- [38] D. Liu and T. Jiang, "Deep reinforcement learning for surgical gesture segmentation and classification," in *International conference on medical image computing and computer-assisted intervention*. Springer, 2018, pp. 247–255.
- [39] X. Gao, Y. Jin, Q. Dou, and P.-A. Heng, "Automatic gesture recognition in robot-assisted surgery with reinforcement learning and tree search," in *2020 IEEE International Conference on Robotics and Automation (ICRA)*. IEEE, 2020, pp. 8440–8446.
- [40] J. Torrents-Barrena, G. Piella, E. Gratacos, E. Eixarch, M. Ceresa, and M. A. G. Ballester, "Deep q-capsnet reinforcement learning framework for intrauterine cavity segmentation in tts fetal surgery planning,"

- IEEE transactions on medical imaging*, vol. 39, no. 10, pp. 3113–3124, 2020.
- [41] M. Chitsaz and W. C. Seng, “Medical image segmentation by using reinforcement learning agent,” in *2009 International Conference on digital Image Processing*. IEEE, 2009, pp. 216–219.
- [42] V. M. Varier, D. K. Rajamani, N. Goldfarb, F. Tavakkolmoghaddam, A. Munawar, and G. S. Fischer, “Collaborative suturing: A reinforcement learning approach to automate hand-off task in suturing for surgical robots,” in *2020 29th IEEE International Conference on Robot and Human Interactive Communication (RO-MAN)*. IEEE, 2020, pp. 1380–1386.
- [43] L. Xie, Y. Miao, S. Wang, P. Blunsom, Z. Wang, C. Chen, A. Markham, and N. Trigoni, “Learning with stochastic guidance for robot navigation,” *IEEE transactions on neural networks and learning systems*, vol. 32, no. 1, pp. 166–176, 2020.
- [44] T. J. Loftus, A. C. Filiberto, Y. Li, J. Balch, A. C. Cook, P. J. Tighe, P. A. Efron, G. R. Upchurch Jr, P. Rashidi, X. Li, *et al.*, “Decision analysis and reinforcement learning in surgical decision-making,” *Surgery*, vol. 168, no. 2, pp. 253–266, 2020.
- [45] T. Nguyen, N. D. Nguyen, F. Bello, and S. Nahavandi, “A new tensioning method using deep reinforcement learning for surgical pattern cutting,” in *2019 IEEE international conference on industrial technology (ICIT)*. IEEE, 2019, pp. 1339–1344.
- [46] C. Sewell, D. Morris, N. H. Blevins, S. Dutta, S. Agrawal, F. Barbagli, and K. Salisbury, “Providing metrics and performance feedback in a surgical simulator,” *Computer Aided Surgery*, vol. 13, no. 2, pp. 63–81, 2008.
- [47] R. Nagyné Elek and T. Haidegger, “Robot-assisted minimally invasive surgical skill assessment—manual and automated platforms,” *Acta Polytechnica Hungarica*, vol. 16, no. 8, pp. 141–169, 2019.
- [48] N. Mirchi, V. Bissonnette, N. Ledwos, A. Winkler-Schwartz, R. Yilmaz, B. Karlik, and R. F. Del Maestro, “Artificial neural networks to assess virtual reality anterior cervical discectomy performance,” *Operative Neurosurgery*, vol. 19, no. 1, pp. 65–75, 2020.
- [49] M. Ershad, R. Rege, and A. M. Fey, “Meaningful assessment of robotic surgical style using the wisdom of crowds,” *International journal of computer assisted radiology and surgery*, vol. 13, no. 7, pp. 1037–1048, 2018.
- [50] H. Liang and M. Y. Shi, “Surgical skill evaluation model for virtual surgical training,” in *Applied Mechanics and Materials*, vol. 40. Trans Tech Publ, 2011, pp. 812–819.
- [51] M. Ershad, R. Rege, and A. M. Fey, “Automatic and near real-time stylistic behavior assessment in robotic surgery,” *International journal of computer assisted radiology and surgery*, vol. 14, no. 4, pp. 635–643, 2019.
- [52] J. Wang, Q. Zhang, D. Zhao, and Y. Chen, “Lane change decision-making through deep reinforcement learning with rule-based constraints,” in *2019 International Joint Conference on Neural Networks (IJCNN)*. IEEE, 2019, pp. 1–6.
- [53] A. P. Wierzbicki and J. Wessels, “The modern decision maker,” in *Model-Based Decision Support Methodology with Environmental Applications*. Springer, 2000, pp. 29–46.
- [54] R. Wen, C.-B. Chng, and C.-K. Chui, “Augmented reality guidance with multimodality imaging data and depth-perceived interaction for robot-assisted surgery,” *Robotics*, vol. 6, no. 2, p. 13, 2017.
- [55] V. Penza, E. De Momi, N. Enayati, T. Chupin, J. Ortiz, and L. S. Mattos, “Envisors: Enhanced vision system for robotic surgery. a user-defined safety volume tracking to minimize the risk of intraoperative bleeding,” *Frontiers in Robotics and AI*, vol. 4, p. 15, 2017.
- [56] F. Cutolo, A. Meola, M. Carbone, S. Sinceri, F. Cagnazzo, E. Denaro, N. Esposito, M. Ferrari, and V. Ferrari, “A new head-mounted display-based augmented reality system in neurosurgical oncology: a study on phantom,” *Computer assisted surgery*, vol. 22, no. 1, pp. 39–53, 2017.
- [57] N. Zevallos, R. A. Srivatsan, H. Salman, L. Li, J. Qian, S. Saxena, M. Xu, K. Patath, and H. Choset, “A surgical system for automatic registration, stiffness mapping and dynamic image overlay,” in *2018 International Symposium on Medical Robotics (ISMR)*. IEEE, 2018, pp. 1–6.
- [58] Y.-Y. Wang, A. Kumar, K.-C. Liu, S.-W. Huang, C.-C. Huang, W.-C. Su, F.-L. Hsiao, and W.-N. Lie, “Stereoscopic augmented reality for single camera endoscopy: a virtual study,” *Computer Methods in Biomechanics and Biomedical Engineering: Imaging & Visualization*, vol. 6, no. 2, pp. 182–191, 2018.
- [59] L. Chen, W. Tang, and N. W. John, “Real-time geometry-aware augmented reality in minimally invasive surgery,” *Healthcare technology letters*, vol. 4, no. 5, pp. 163–167, 2017.
- [60] M. S. Nosrati, R. Abugharbieh, J.-M. Peyrat, J. Abinahed, O. Al-Alao, A. Al-Ansari, and G. Hamarneh, “Simultaneous multi-structure segmentation and 3d nonrigid pose estimation in image-guided robotic surgery,” *IEEE Transactions on Medical Imaging*, vol. 35, no. 1, pp. 1–12, 2016.
- [61] K. S. Tang, D. L. Cheng, E. Mi, and P. B. Greenberg, “Augmented reality in medical education: a systematic review,” *Canadian medical education journal*, vol. 11, no. 1, p. e81, 2020.
- [62] A. M. Jarc, A. A. Stanley, T. Clifford, I. S. Gill, and A. J. Hung, “Proctors exploit three-dimensional ghost tools during clinical-like training scenarios: a preliminary study,” *World journal of urology*, vol. 35, no. 6, pp. 957–965, 2017.
- [63] “da vinci research kit research wiki page,” Website, 2021, https://research.intusurg.com/index.php/Main_Page.
- [64] H. Lin, C.-W. V. Hui, Y. Wang, A. Deguet, P. Kazanzides, and K. S. Au, “A reliable gravity compensation control strategy for dvrk robotic arms with nonlinear disturbance forces,” *IEEE Robotics and Automation Letters*, vol. 4, no. 4, pp. 3892–3899, 2019.
- [65] J. Xu, B. Li, B. Lu, Y.-H. Liu, Q. Dou, and P.-A. Heng, “Surrol: An open-source reinforcement learning centered and dvrk compatible platform for surgical robot learning,” *arXiv preprint arXiv:2108.13035*, 2021.
- [66] B. Lu, W. Chen, Y.-M. Jin, D. Zhang, Q. Dou, H. K. Chu, P.-A. Heng, and Y.-H. Liu, “A learning-driven framework with spatial optimization for surgical suture thread reconstruction and autonomous grasping under multiple topologies and environmental noises,” in *2020 IEEE/RSJ International Conference on Intelligent Robots and Systems (IROS)*. IEEE, 2020, pp. 3075–3082.
- [67] W. J. Hyung and Y. Woo, “Tilepro,” in *Robotics in General Surgery*. Springer, 2014, pp. 457–460.
- [68] M. Andrychowicz, F. Wolski, A. Ray, J. Schneider, R. Fong, P. Welinder, B. McGrew, J. Tobin, P. Abbeel, and W. Zaremba, “Hindsight experience replay,” in *Proceedings of the 31st International Conference on Neural Information Processing Systems*, 2017, pp. 5055–5065.
- [69] A. Tabb and K. M. A. Yousef, “Solving the robot-world hand-eye (s) calibration problem with iterative methods,” *Machine Vision and Applications*, vol. 28, no. 5, pp. 569–590, 2017.
- [70] R. Y. Tsai, R. K. Lenz, *et al.*, “A new technique for fully autonomous and efficient 3 d robotics hand/eye calibration,” *IEEE Transactions on robotics and automation*, vol. 5, no. 3, pp. 345–358, 1989.
- [71] F. C. Park and B. J. Martin, “Robot sensor calibration: solving $ax=xb$ on the euclidean group,” *IEEE Transactions on Robotics and Automation*, vol. 10, no. 5, pp. 717–721, 1994.
- [72] L. Qian, T. Song, M. Unberath, and P. Kazanzides, “Ar-loupe: Magnified augmented reality by combining an optical see-through head-mounted display and a loupe,” *IEEE Transactions on Visualization and Computer Graphics*, 2020.
- [73] Z. Zhang, “A flexible new technique for camera calibration,” *IEEE Transactions on pattern analysis and machine intelligence*, vol. 22, no. 11, pp. 1330–1334, 2000.
- [74] V. Lepetit, F. Moreno-Noguer, and P. Fua, “Epnnp: An accurate o (n) solution to the pnp problem,” *International journal of computer vision*, vol. 81, no. 2, p. 155, 2009.
- [75] R. A. Joseph, A. C. Goh, S. P. Cuevas, M. A. Donovan, M. G. Kauffman, N. A. Salas, B. Miles, B. L. Bass, and B. J. Dunkin, ““chopstick” surgery: a novel technique improves surgeon performance and eliminates arm collision in robotic single-incision laparoscopic surgery,” *Surgical endoscopy*, vol. 24, no. 6, pp. 1331–1335, 2010.
- [76] K. Koide and E. Menegatti, “General hand-eye calibration based on reprojection error minimization,” *IEEE Robotics and Automation Letters*, vol. 4, no. 2, pp. 1021–1028, 2019.
- [77] R. B. Miller, “Response time in man-computer conversational transactions,” in *Proceedings of the December 9-11, 1968, fall joint computer conference, part I*, 1968, pp. 267–277.
- [78] N. Tolia, D. G. Andersen, and M. Satyanarayanan, “Quantifying interactive user experience on thin clients,” *Computer*, vol. 39, no. 3, pp. 46–52, 2006.